

## Cohesive Zone Modeling of Mode I Fracture in Adhesive Bonded Joints

M. Alfano<sup>1,2</sup>, F. Furgiuele<sup>1</sup>, A. Leonardi<sup>1</sup>, C. Maletta<sup>1</sup> and G. H. Paulino<sup>2</sup>

<sup>1</sup>Department of Mechanical Engineering, University of Calabria, 87036 Arcavacata di Rende, Italy

<sup>2</sup>Department of Civil and Environmental Engineering, University of Illinois at Urbana-Champaign, Newmark Laboratory, 205 N. Mathews Avenue, Urbana, IL 61801-2352, U.S.A.

e-mail: [alfano@unical.it](mailto:alfano@unical.it)

**Keywords:** Mode I fracture; cohesive zone model (CZM); nonlinear fracture; adhesive joints.

### Abstract.

This paper deals with the application of Cohesive Zone Model (CZM) concepts to study mode I fracture in adhesive bonded joints. In particular, an intrinsic piece-wise linear cohesive surface relation is used in order to model fracture in a pre-cracked bonded Double Cantilever Beam (DCB) specimen. Finite element implementation of the CZM is accomplished by means of the user element (UEL) feature available in the FE commercial code ABAQUS. The sensitivity of the cohesive zone parameters (*i.e.* fracture strength and critical energy release rate) in predicting the overall mechanical response is first examined; subsequently, cohesive parameters are tuned comparing numerical simulations of the load-displacement curve with experimental results retrieved from literature.

### Introduction

Adhesive joints are a subject of great interest in different fields (*e.g.* automotive, aerospace, biomedical, microelectronics, etc) because of the advantages they provide with respect to the traditional joining techniques, *e.g.* less sources of stress concentration, more uniform load distribution, weight reduction and major flexibility in design. The strength properties of adhesive bonded joints are most commonly evaluated by standard test methods assuming a defect free bond-line; however, inaccurate joint fabrication or inappropriate curing may cause the occurrence of bubbles, dust particles and un-bonded areas [1].

Therefore, the use of adhesive joints in critical structural applications necessitates the developments of robust integrity assessment methodologies and testing procedures in order to tackle fracture events. A valuable approach for analyzing the fracture properties of adhesive bonded joints is represented by the Linear Elastic Fracture Mechanics (LEFM) [2-7]. It requires pre-existing crack like flaws and, therefore, nucleation of these flaws cannot be treated directly. Furthermore, it neglects a detailed description of what happens in the fracture process zone because it lumps all effects into the crack tip; however, a detailed description of the fracture process zone is essential, especially to understand fracture mechanisms and to design suitable modifications of the material (*e.g.* toughening by reinforcement in polymeric structural adhesive [8]). From this standpoint, a powerful and efficient computational tool for fracture studies, that allows to overcome the limitations mentioned above, is represented by Cohesive Zone Model (CZM) of fracture. By means of CZM, crack initiation and growth are obtained as a natural part of the solution without *a priori* or *ad hoc* assumptions. So far, CZM has been successfully applied to model fracture in metals, concrete, polymers and functionally graded materials (FGMs) [9-16].

In the present study, CZM has been used in order to investigate fracture behavior in a pre-cracked double cantilever beam (DCB). In particular, finite element implementation of four nodes cohesive surface elements is accomplished using the UEL feature available in the FE commercial code ABAQUS [17]. The sensitivity of the cohesive zone parameters (*i.e.* fracture strength and critical energy release rate) in predicting the overall mechanical response is first examined; subsequently, these parameters are tuned comparing numerically simulated load-displacement curves with experimental results retrieved from literature [6].

### Cohesive Zone Model (CZM)

**CZM concept.** The standard model used to describe the crack tip process zone assumes bonds stretching orthogonal to the crack surfaces until they break at a characteristic stress level. Thus, the singular region introduced from LEFM can be replaced by a lateral region over which non-linear phenomena occur. This model evolved from the Dugdale-Barenblatt process zone [18,19]. According to CZM, the fracture process is lumped into the crack line and is characterized by a cohesive law that relates tractions and displacements jump across cohesive surfaces (T- $\Delta$ ). In the simplest and most usual formulation of CZM, the whole body volume remains elastic while the nonlinearity is embedded in the cohesive law which dictates the interfacial conditions along the crack line (Fig. 1). The peak stress on the cohesive law is the cohesive strength of the material,  $\sigma_c$ , while the area under the curve is the cohesive fracture energy,  $G_c$ . As a consequence, fracture process can be summarized as illustrated in Fig. 1: at first a linear elastic material response prevails (1), as the load increases the crack initiates ( $T=\sigma_c$ ) (2) and then, governed by the non linear cohesive law, it evolves from initiation to complete failure (3) with the appearance of new traction free crack surfaces ( $\Delta=\Delta_c$ ) (4).

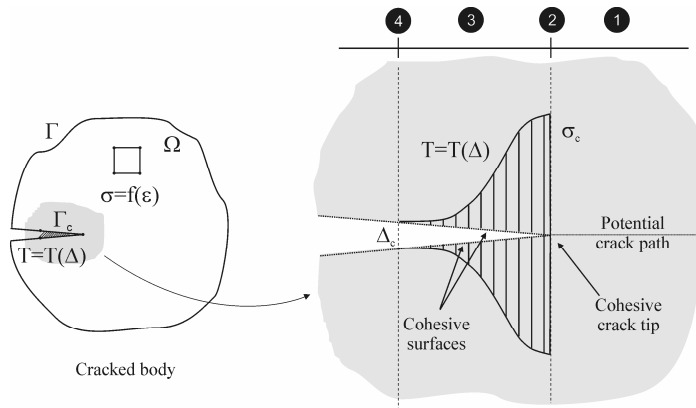


Fig. 1. Cohesive zone modeling of fracture

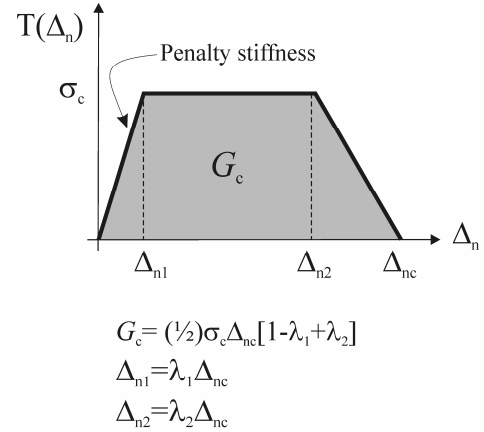


Fig. 2. Cohesive law

Therefore, the continuum should be characterized by two constitutive laws; for instance, a linear stress-strain relation for the bulk material and a cohesive surface relation (cohesive law) that allows crack spontaneous initiation and growth. To this aim, it is important to properly select the shape of the softening curve. In the present paper the piece-wise linear traction-separation law shown in Fig. 2 [20] has been adopted in order to investigate mode I fracture in adhesive bonded joints. As it can be seen, for this particular (T- $\Delta$ ) curve, the governing cohesive parameters are the cohesive fracture energy ( $G_c$ ), the peak stress ( $\sigma_c$ ), the critical opening displacement ( $\Delta_{nc}$ ) and the factors  $\lambda_1$  and  $\lambda_2$  whose values dictate the shape of  $T=T(\Delta_n)$ .

**Finite element implementation.** The cohesive view of fracture is captured by surface constitutive relations that describe the evolution of tractions (T) generated across the faces of a crack as a function of the crack face displacements jump ( $\Delta$ ). Therefore, implementation of cohesive zone in FEM framework requires bulk finite elements, for modeling the stage (1) in Fig.1, bordered by cohesive surface elements for the remaining three stages: (2) crack initiation, (3) crack evolution and (4) complete failure. The insertion of cohesive surface elements bridges linear elastic and fracture behavior allowing for spontaneous crack propagation. In a variational setting, the principle of virtual work including the contribution of cohesive surfaces is given as follows:

$$\int_{\Omega} \boldsymbol{\sigma} : \boldsymbol{\varepsilon}^* d\Omega - \int_{\Gamma_c} \mathbf{T} \cdot \boldsymbol{\Delta}_n^* d\Gamma_c - \int_{\Gamma} \mathbf{P} \cdot \mathbf{u}^* d\Gamma = 0 \quad (1)$$

where  $\boldsymbol{\varepsilon}^*$  is the virtual strain associated to the virtual displacement  $\mathbf{u}^*$  defined in the domain  $\Omega$ ;  $\boldsymbol{\Delta}_n$  denotes the virtual crack faces normal displacement jump along the crack line  $\Gamma_c$ ;  $\mathbf{T}$  is the traction

vector along the cohesive zone;  $\mathbf{P}$  is the external traction vector (see Fig.1). The first term in Eq. (1) is the internal virtual work for bulk elements while the contribution of cohesive surface elements to the internal virtual work is represented by the second integral. Exploiting the finite element formulation, we can rewrite Eq. 1 as

$$\left[ \int_{\Omega} \mathbf{B}^T \mathbf{E} \mathbf{B} d\Omega - \int_{\Gamma_c} \mathbf{N}_c^T \frac{\partial \mathbf{T}}{\partial \Delta_n} \mathbf{N}_c d\Gamma_c \right] \mathbf{d} = \int_{\Gamma} \mathbf{N}^T \mathbf{P} d\Gamma \quad (2)$$

where  $\mathbf{N}$  and  $\mathbf{N}_c$  are matrices of the shape functions for bulk and cohesive elements, respectively,  $\mathbf{B}$  is the derivative of  $\mathbf{N}$ ,  $\mathbf{d}$  are the nodal displacements,  $\mathbf{E}$  is the tangential stiffness matrix for the bulk elements, and  $\partial \mathbf{T} / \partial \Delta_n$  is the Jacobian stiffness matrix. Therefore, in order to carry out the iterations of the method [17], the contribution of cohesive elements to the tangent stiffness matrix as well as to the force vector is acquired from the numerical implementation of the CZM. Four nodes cohesive zone elements have been implemented within the commercial FE code ABAQUS (version 6.5-1) using the UEL capability. The piece-wise linear traction-separation law showed in the previous section has been adopted. A detailed description of element formulation is reported elsewhere [21,22].

### Simulation of fracture in DCB configuration

The specimen analyzed herein is the DCB studied in [6]. A schematic representation is reported in Fig. 3 together with geometrical dimensions and mechanical properties of the materials. The measured fracture toughness reported in [6] is  $G_c = 550$  N/m. A finite element model of this test configuration was obtained using ABAQUS; about 9500 four nodes linear isoparametric elements were used for the bulk material and about 200 cohesive elements for the cohesive zone, *i.e.* the bond-line.

A sensitivity analysis to cohesive fracture parameters has been performed. According to what reported in [20], the influence of T- $\Delta$  law shape on the simulated mechanical responses is relatively weak as compared to other cohesive parameters, *i.e.* material strength ( $\sigma_c$ ) and cohesive fracture energy ( $G_c$ ). Therefore, for the sensitivity analysis,  $\lambda_1$  and  $\lambda_2$  have been fixed to 0.15 and 0.5, respectively.

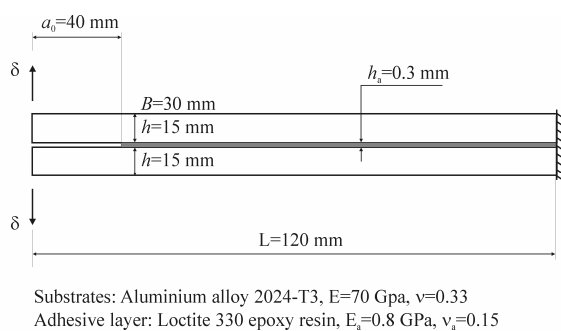


Fig. 3. Schematic representation of the specimen

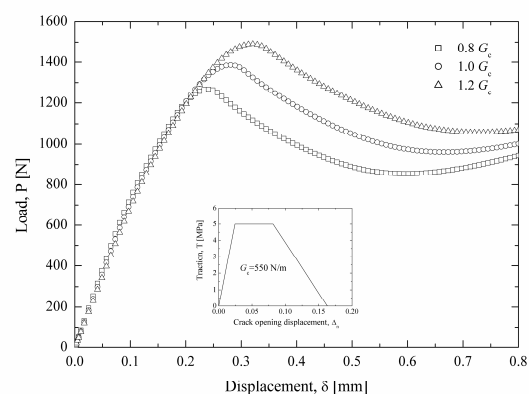


Fig. 4. Sensitivity to cohesive fracture energy ( $G_c$ )

Fig. 4 illustrates the sensitivity of  $P$  versus the opening displacement  $\delta$  curve to different fracture energies, *i.e.*  $1.2G_c$ ,  $G_c$  and  $0.8G_c$ . The cohesive strength,  $\sigma_c$  was held constant and equal to 5 MPa. As it can be seen, as the fracture energy increases the area under the curve (global fracture energy) and the peak load are increased. Fig. 5 shows the sensitivity to different cohesive strengths, *i.e.*  $1.2\sigma_c$ ,  $\sigma_c$  and  $0.8\sigma_c$ . In this case, the value of the cohesive fracture energy was held fixed and equal to 550 N/m. As the critical strength increases the peak load is increased while the global fracture energy is almost constant. The parameters of the cohesive zone model are then tuned in order to match the experimental results reported in [6]. As it can be seen from Fig. 6, the cohesive

parameters that give minimum deviations between numerical and experimental P- $\delta$  curves are:  $G_c=550$  N/m,  $\sigma_c=4$  MPa,  $\lambda_1=0.01$  and  $\lambda_2=0.5$ .

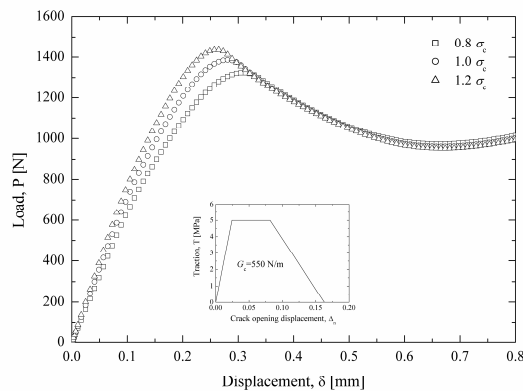


Fig. 5. Sensitivity to cohesive strength

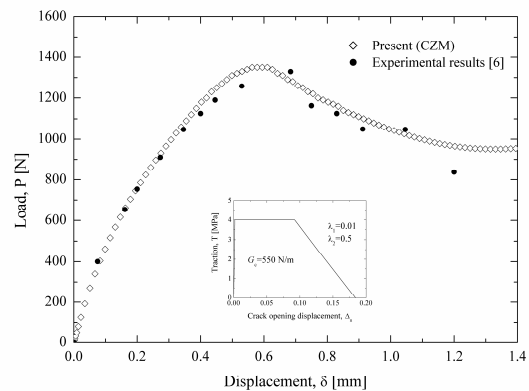


Fig. 6. Experimental and numerical P- $\Delta$  curve

## Summary and conclusions

In this paper, Cohesive Zone Model (CZM) concepts were applied in order to study mode I fracture in a pre-cracked bonded Double Cantilever Beam (DCB) specimen. A cohesive surface element has been implemented in a finite element commercial code (ABAQUS UEL) using an intrinsic piecewise linear cohesive law. The sensitivity of cohesive zone parameters (*i.e.* fracture strength and critical energy release rate) in predicting the overall mechanical response has been examined. In addition, cohesive parameters were identified comparing numerically simulated load-displacement curves with experimental data retrieved from the literature. A good agreement between both solutions has been observed.

## References

- [1] A.J. Kinloch: Adhesion and Adhesives, Science and Technology, Chap. & Hall, London 1986.
- [2] H. Chai: J Mat Sci Letters, Vol. 7 (1988), p. 399.
- [3] A.R. Akisanya, N.A. Fleck: Int J Fracture, Vol. 58 (1992), p. 93.
- [4] A.R. Akisanya, N.A. Fleck: Int J Fracture, Vol. 55 (1992), p. 29.
- [5] B. Chen, D.D. Dillard, J.G. Dillard, R.L. Clark: Int J Fracture, Vol. 114 (2002), p. 167.
- [6] A. Pironi, G. Nicoletto: Proc. of the Italian Group of Fracture, Bari, 2000. (in Italian)
- [7] M. Alfano, F. Furgiuele, C. Maletta: Key Eng Mat, Vol. 325 (2006), p.149.
- [8] J.G. Williams, Fracture Mechanics of Polymers, Halsted Press, John Wiley & Sons, NY, 1984.
- [9] W. Li, T. Siegmund: Eng Fract Mech, Vol. 69 (2002), p.2073.
- [10] J.R. Roesler, G.H. Paulino, K. Park, C. Gedicke: Cem & Concr Comp, Vol. 29 (2007), p.300
- [11] S.H. Song, G. H. Paulino, W.G. Buttlar: ASCE J Eng Mech, Vol. 132 (2006), p.1215.
- [12] S.H. Song, G. H. Paulino, W.G. Buttlar: Eng Fract Mech, Vol. 73 (2006), p.2829.
- [13] Z. Jin, G.H. Paulino, R.H. Dodds Jr.: Eng. Fract Mech, Vol. 70 (2003), p. 1885.
- [14] Z. Zhang, G.H. Paulino: Int J Plasticity, Vol. 21 (2006), p 1195
- [15] D. -J. Shim, G.H. Paulino, R.H. Dodds Jr.: Int J Fracture, Vol. 139 (2006), p. 91
- [16] Z. Zhang, G.H. Paulino: Int J Solids and Struct, (in press)
- [17] ABAQUS User's Manual, v6.5-1. Pawtucket, USA, Hibbit, HKS Inc; 2002.
- [18] Dugdale D.S.: J. Mech. Phys. Solids, Vol. 8 (1960), p.100.
- [19] Barrenblatt G.I.: Adv. Appl. Mech., Vol. 7 (1962), p.55
- [20] V. Tvergaard, J. W. Hutchinson: J Mech Phys. Solids, Vol. 40, p. 1377.
- [21] K. Park, MSc thesis, University of Illinois at Urbana-Champaign, 2005
- [22] M. Alfano, Technical Report, University of Illinois at Urbana-Champaign, 2006.